HYDROLOGICAL PROCESSES
Hydrol. Process. (2012)
Published online in Wiley Online Library
(wileyonlinelibrary.com) DOI: 10.1002/hyp.9677

Response of hydrology to climate change in the southern Appalachian Mountains using Bayesian inference

Wei Wu,[1*,†] James S. Clark[1] and James M. Vose[2‡]

[1] *Nicholas School of the Environment, Duke University, Box 90328, Durham, NC 27708, USA*
[2] *USDA-Forest Service, Coweeta Hydrologic Laboratory, 3160 Coweeta Lab Road, Otto, NC 28763, USA*

Abstract:

Predicting long-term consequences of climate change on hydrologic processes has been limited due to the needs to accommodate the uncertainties in hydrological measurements for calibration, and to account for the uncertainties in the models that would ingest those calibrations and uncertainties in climate predictions as basis for hydrological predictions. We implemented a hierarchical Bayesian (HB) analysis to coherently admit multiple data sources and uncertainties including data inputs, parameters, and model structures to identify the potential consequences of climate change on soil moisture and streamflow at the head watersheds ranging from low to high elevations in the southern Appalachian region of the United States. We have considered climate change scenarios based on three greenhouse gas emission scenarios of the Interovernmental Panel on Climate Change: A2, A1B, and B1 emission scenarios.

Full predictive distributions based on HB models are capable of providing rich information and facilitating the summarization of prediction uncertainties. With predictive uncertainties taken into account, the most pronounced change in soil moisture and streamflow would occur under the A2 scenario at both low and high elevations, followed by the A1B scenario and then by the B1 scenario. Uncertainty in the change of soil moisture is less than that of streamflow for each season, especially at high elevations. A reduction of soil moisture in summer and fall, a reduction or slight increase of streamflow in summer, and an increase of streamflow in winter are predicted for all three scenarios at both low and high elevations.

The hydrological predictions with quantified uncertainties from a HB model could aid more-informed water resource management in developing mitigation plans and dealing with water security under climate change. Copyright © 2012 John Wiley & Sons, Ltd.

Supporting information may be found in the online version of this article.

KEY WORDS hierarchical Bayesian models; hydrological models; climate change; streamflow; soil moisture

Received 12 June 2012; Accepted 23 November 2012

INTRODUCTION

Global climate change will generally have a net negative impact on water resources (Kundzewicz *et al.*, 2007; Gosling *et al.*, 2011; Sivakumar, 2011). Temperature increases will intensify the hydrological cycle, and extremes (floods and droughts) are likely to increase in frequency and magnitude (Jackson *et al.*, 2001; Gedney *et al.*, 2006; Oki and Kanae, 2006; Chiew *et al.*, 2011; Sivakumar, 2011). Risks of extreme hydrological events depend not only on the possible changes in climate in the future, but also on the current status of the hydrological conditions, and they vary by region (Groisman and Knight, 2008). In the US, a simple reduction in total annual precipitation might increase drought severity in the 'annual, seasonal drought' regions which are dependent on dormant season precipitation and soil recharge, but it would not have the same impact on forests of the 'random, occasional drought' regions of the eastern US (Penninckx *et al.*, 1999; Hanson and Weltzin, 2000). Temperate regions will likely experience summer drying from increased evapotranspiration, lower summer precipitation, or both (Gleick, 1987; Neilson and Marks, 1994; Jackson *et al.*, 2001; Loukas *et al.*, 2002; Kilsby *et al.*, 2007). Tropical regions may experience smaller warming-induced changes in the hydrological cycle (IPCC, 1996; Jackson *et al.*, 2001). In an integrated assessment of 50-year runoff events (Q_{50y}) based on one climate change scenario for some of the largest river basins in the world, the changes were found to be heterogeneous (Kleinen and Petschel-Held, 2007). The Q_{50yr} was predicted to increase markedly in the Amazon, Parana, Chang Jiang, and Mekong basins, but decrease markedly in Mississippi, Amur, Mackenzie, and Danube river basins (Kleinen and Petschel-Held, 2007).

The capacity to anticipate how water resources will be affected by climate change is critical for development of mitigation and adaption strategies that can sustain water resources and minimize environmental, economic, and social costs related to water shortages and floods (Vörösmarty *et al.*, 2000; Jackson *et al.*, 2001; Meybeck and Vörösmarty, 2004; Barnett *et al.*, 2008; Palmer *et al.*, 2008). However, anticipating the long-term consequences of climate change has been challenging, in part, by the dual needs to accommodate the uncertainties in the precipitation, temperature, soil moisture, and streamflow data used for calibration, and to account for the uncertainties in the models that would ingest those calibrations as basis for

*Correspondence to: Wei Wu, Department of Coastal Sciences, the University of Southern Mississippi, 703 East Beach Drive, Ocean Springs, MS 39564
E-mail: wei.wu@usm.edu
†Current Address: Department of Coastal Sciences, the University of Southern Mississippi, 703 East Beach Drive, Ocean Springs, MS 39564.
‡Current Address: Center for Integrated Forest Science and Synthesis, USDA Forest Service Southern Research Station, North Carolina State University, Box 8008, Raleigh, NC 27695, USA.

prediction (Clark *et al*., 2001; Schneider, 2001). In addition, analysis requires integration of predictions derived from climate models, most commonly assessed at regional or global scales over seasons to decades with finer scale (catchment runoff) and fast (hour to daily precipitation and evapotranspiration) data. Uncertainties at regional scales under climate change include inherent unpredictability of precipitation, which depends on sub-grid processes in climate models, and incomplete understanding of changes of evapotranspiration, which is driven by processes that are often poorly characterized in hydrologic models, such as stomatal closure influenced by elevated CO_2 concentrations and interactions involving energy transfer with complex surface and vegetation (Ohmura and Wild, 2002; Oki and Kanae, 2006). The many variables that control runoff are likewise typically crudely parameterized in hydrologic models (Jakeman and Hornberger, 1993; Kuczera and Mroczkowski, 1998).

Improved hydroclimate projections, with reliable probabilistic quantification of uncertainties, would lead to more-informed water resource management decisions (Chiew *et al*., 2011; Sivakumar, 2011). However, many hydrologic models do not readily permit coherent assimilation of the multiple sources data and uncertainties needed to generate probabilistic predictions. In many models, inputs, intermediates, and outputs are deterministic transformations of one another, thus precluding model uncertainty. Most do not accommodate unknowns and poorly quantified variables. Complexity and limited understanding of processes that control hydrologic cycles suggest that models should be stochastic at the 'process level' (Wikle, 2003; Clark *et al*., 2011). This allows conditional independence at the 'data' stage, taking up the relationships among state variables at the 'process' stage, still tractable when decomposed into a hierarchical structure (Wu *et al*., 2010). Hierarchical Bayes represents such a hierarchical modeling structure that can deal with the complexity and uncertainty at multiple stages and multiple data sources (Clark, 2005). Therefore, it shows a promising tool in hydrology (e.g. Krzysztofowicz, 1999; Vrugt and Robinson, 2007; Ajami *et al*., 2007). Implementation of hierarchical Bayesian (HB) model and more generally Bayesian inference in hydrological studies has been made feasible by recent advances in computation, i.e. Metropolis or Metropolis–Hasting algorithm in Markov chain Monte Carlo (MCMC) simulation (Kuczera and Parent, 1998; Campbell *et al*., 1999; Bates and Campbell, 2001), differential evolution Markov Chain with snooker updater (ter Braak and Vrugt, 2008), adaptive Metropolis–Hasting steps (Haario *et al*., 2001; Marshall *et al*., 2004; Wu *et al*., 2010), sequential Monte Carlo sampling such as ensemble Kalman filter (Vrugt *et al*., 2005), and particle MCMC algorithm which combines the strengths of sequential data assimilation and MCMC simulation (Vrugt *et al*., 2012).

In this study, we predict the potential consequences for hydrology under climate change by the end of the century, with a coherent assimilation of hydrological models and multiple data sources using a HB analysis, at forested headwater streams in the Little Tennessee River of northeast Georgia and western North Carolina.

METHODS

Site description and data

Our study areas are Watersheds 18 and 27 (Figure S1), reference watersheds at the USDA Forest Service, Coweeta Hydrologic Laboratory located in the Nantahala Mountain Range of western North Carolina within the Blue Ridge Physiographic Province (35º03'N, 83º25'W). The Coweeta Basin (1626 ha) has been a center of forest hydrological research in the mountains-piedmont of Georgia, South Carolina, North Carolina, and Virginia since 1934, and it has been a National Science Foundation Long-Term Ecological Research Site since 1980 (Swank and Crossley, 1988). Climate at Coweeta Basin is marine humid temperate and characterized by cool summers, mild winters, and abundant rainfall in all seasons (Swift *et al*., 1988). Average annual precipitation varies from 1700 mm at low elevations (680 m) to 2500 mm on upper slopes (>1400 m). It is dominated by rain events with less than 5% being snow. The underlying bedrock is the Coweeta group (Hatcher, 1979), which consists of quartz diorite gneiss, metasandstone and peltic schist, and quartzose metasandstone (Hatcher, 1988). The regolith of the Coweeta basin is deeply weathered and averages about 7 m in depth.

Watershed 18 (WS18 12.5 ha) and watershed 27 (WS27 38.8 ha) have been unmanaged since selective logging in the early 1900s. The vegetation in both watersheds is mixed hardwoods. The elevation of Watershed 18 (referred as low-elevation watershed) ranges from 726 to 993 m.a.s.l with an average slope of 52 and aspect of north-east. Watershed 27 (referred as high-elevation watershed) has elevation from 1061 to 1454 m.a.s.l with an average slope of 55 and aspect of north-north-east. It was partially defoliated by fall crankerworm infestation from 1975 to 1979.

The data used in the study include precipitation, temperature, soil moisture, and streamflow at a daily time step. Daily precipitation and temperature data came from rain gauges and climate stations located within or near the watersheds. Daily soil moisture data came from long-term monitoring data at representative plots at terrestrial gradient sites within WS18 and WS27. Streamflow data came from the stream gauges at the outlets of WS18 and WS27.

Baseline and climate change scenarios

For the baseline scenario, we use climate data from 1984 to 2004 at low elevations and from 1992 to 2004 at high elevations. Due to the large uncertainties in climate change predictions, we considered three greenhouse gas emission scenarios of Intergovernmental Panel on Climate Change (IPCC): a continual increasing rate of emission over the 21st century (A2), a mid-21st century leveling-off of emission (A1B), and a global curbing of emissions over the 21st century (B1) (Nakiénovic *et al*., 2000; Girvetz *et al*., 2009). These scenarios differ in the predictions of population, world gross domestic production, per capita income ratio

DOI: 10.1002/hyp

(developed countries and economic in transition to developing countries), technology innovation rates, etc. (Nakiénovic *et al.*, 2000). We obtained the World Climate Research Programme's (WCRP's) Coupled Model Intercomparison Project Phase 3 (CMIP3) multi-model dataset for the three emission scenarios (available at www.climatewizard.org, accessed on April 6, 2012). We used the quantiles and mean of ensemble predictions of changes in seasonal temperature and precipitation for 2070–2099 in reference to 1961–1990 downscaled (horizontal spatial resolution: 12 km) from 16 global circulation models (Table I). The quantiles include ensemble minimum, 20%, 40%, 60%, 80% quantiles, and maximum. We fitted Gaussian distributions by moment matching with mean and variance (Equation 1):

$$\hat{\mu} = \sum_q p_q T_q \Big/ \sum_q p_q$$
$$\hat{v} = \sum_q p_q T_q^2 \Big/ \sum_q p_q - \hat{\mu}^2 \quad (1)$$

for temperature T_q and percentage p_q at quantile q. The same method was used for precipitation. Then, we randomly sampled from the normal distribution truncated at minimum and maximum values to derive changes in temperature and precipitation in each season under the climate change scenarios using msm (multi-state Markov and hidden Markov models in continuous time) package (Jackson, 2011) in R (R Development Core Team, 2008).

Process model

We applied a parsimonious daily lumped rainfall-runoff model with quick and slow flow components 'GR4J' (Modele du Genie Rural a 4 parametres Journalier) (Perrin *et al.*, 2003; Wu *et al.*, 2010), but allowed for error at this process level (Wu *et al.*, 2010). The parsimonious model has four parameters: the maximum capacity of soil moisture storage (k_1), a ground water exchange coefficient (k_2), the maximum capacity of routing storage (k_3), and a time base of a unit hydrograph (k_4) (i.e. time of concentration of a watershed, defined as time required for water to travel from the most hydraulically remote point in the basin to the basin outlet). The model can be divided into four submodels: a soil moisture submodel, an effective precipitation (the proportion of precipitation that could contribute to streamflow) submodel, a non-linear routing slow streamflow submodel, and a non-routing quick streamflow submodel. Stochaosity in processes was accommodated in the soil moisture submodel and the combined non-routing and routing submodels.

HB model

Our hierarchical model structure was designed to estimate the components of streamflow generation, including the parameters, latent states of soil moisture and streamflow, and uncertainties of the inputs, parameters, and model structures (Wu *et al.*, 2010). We assumed the major uncertainties of the model include simulations in soil moisture and streamflow (termed 'model misspecification' or 'process error'). Thus, the submodels for soil moisture, slowflow, and quickflow were stochastic, while the submodel of effective precipitation was treated deterministically. We also considered the effects of sampling or observation errors for the measurements of precipitation, soil moisture, and streamflow. We used priors that were conjugate with the

Table I. The ensemble quantiles of changes in temperature and precipitation from CMIP3 dataset

Variables	Scenario	Season	Minimum	20%	40%	Mean	60%	80%	Maximum
Air Temperature (unit: °F)	A2	Spring	3.71	5.35	7.20	7.27	7.53	7.64	9.36
		Summer	4.09	6.00	7.35	7.47	7.88	10.90	11.49
		Fall	4.50	6.04	7.50	7.56	7.77	8.50	10.81
		Winter	2.92	4.80	5.11	5.34	5.59	6.33	8.68
	A1B	Spring	3.11	5.12	5.86	6.20	6.23	7.18	7.84
		Summer	4.36	5.21	6.37	6.75	7.25	8.05	9.41
		Fall	4.17	5.50	6.26	6.37	6.85	7.58	9.40
		Winter	2.23	4.40	4.60	4.69	4.73	6.94	7.97
	B1	Spring	1.76	3.34	3.94	4.26	4.49	5.18	5.62
		Summer	2.23	3.21	4.15	4.52	5.09	5.31	6.73
		Fall	2.52	3.02	4.39	4.74	4.93	5.26	5.83
		Winter	1.19	2.69	3.48	3.58	3.76	4.61	6.06
Precipitation (%)	A2	Spring	−20.20	−2.63	−0.142	3.22	5.39	15.71	21.63
		Summer	−36.37	−9.80	−0.445	3.41	5.02	19.98	49.28
		Fall	−18.08	−7.37	−0.466	6.68	10.22	16.69	32.95
		Winter	−28.51	−6.68	1.26	4.42	8.30	16.67	35.22
	A1B	Spring	−18.73	0.159	5.50	6.47	7.31	12.21	28.24
		Summer	−27.88	−10.96	−3.30	3.30	11.21	24.35	43.67
		Fall	−14.15	−2.61	2.98	5.73	6.89	14.33	19.07
		Winter	−15.06	−7.37	−1.26	1.69	8.35	19.01	30.73
	B1	Spring	−10.61	−2.83	1.07	3.87	5.16	13.19	21.80
		Summer	−14.49	−7.16	2.26	4.41	5.49	14.97	31.61
		Fall	−11.52	−2.86	2.23	3.18	4.21	11.70	27.67
		Winter	−22.07	−6.31	−0.642	4.20	8.52	13.93	17.60

DOI: 10.1002/hyp

likelihood (Calder *et al*., 2003), so that prior and posterior distribution had the same form, thus facilitating mixing of Markov chains.

Combining the data, process, and parameter models, we have the joint posterior (Equation 2, Wu *et al*., 2010, Figure S2):

$$
\begin{aligned}
&p(k_1,k_2,k_3,k_4,\boldsymbol{s},\boldsymbol{q},\sigma_1^2,\sigma_2^2,\tau_1^2,\tau_2^2,\tau_p^2\,|\,\boldsymbol{p}^o,\boldsymbol{temp},\boldsymbol{y},\boldsymbol{z},priors)\\
&\propto \prod_{t=1}^{T} N(\boldsymbol{y}_t\,|\,\boldsymbol{q}_t,\tau_1^2)\prod_{t=1}^{T} N(\boldsymbol{z}_t|\boldsymbol{s}_t,\tau_2^2)\\
&\prod_{t=1}^{T} N(\boldsymbol{q}_t|f_1(\boldsymbol{s}_t,k_2,k_3,k_4),\sigma_1^2)\\
&\prod_{t=2}^{T} N(\boldsymbol{s}_t|f_2(\boldsymbol{s}_{t-1},\boldsymbol{p}_t,\boldsymbol{temp}_t,k_1),\sigma_2^2)\\
&\prod_{t=1}^{T} N(\log(\boldsymbol{p}_t^o)|\log(\boldsymbol{p}_t),\tau_p^2)\\
&N(\log(k_1,k_2,k_3,k_4)|\log(B),diagnoal(V_B))\\
&IG(\sigma_1^2|\alpha_{\sigma_1^2},\beta_{\sigma_1^2})\\
&IG(\sigma_2^2|\alpha_{\sigma_2^2},\beta_{\sigma_2^2})\\
&IG(\tau_1^2|\alpha_{\tau_1^2},\beta_{\tau_1^2})\\
&IG(\tau_2^2|\alpha_{\tau_2^2},\beta_{\tau_2^2})\\
&IG(\tau_p^2|\alpha_{\tau_p^2},\beta_{\tau_p^2})
\end{aligned}
\tag{2}
$$

where N is the normal distribution, log represents natural logarithm, IG is the inverse gamma distribution, k_1–k_4 are the four parameters in the GR4J model: k_1 denotes the maximum capacity of soil moisture storage, k_2 denotes a ground water exchange coefficient, k_3 denotes the maximum capacity of routing storage, and k_4 denotes a time base of a unit hydrograph, **s** denotes true soil moisture content, **q** denotes true log streamflow, **p** denotes true precipitation, σ_1^2 denotes lognormal variance in combined slow flow and quick flow submodels, σ_2^2 denotes normal variance in soil moisture submodel, τ_1^2 denotes lognormal observation variance for streamflow measurements, τ_2^2 denotes normal observation variance for soil moisture measurements, τ_p^2 denotes lognormal observation varaince for precipitation measurements, $\mathbf{p}^o$ denotes observed precipitation, **temp** denotes temperature, **y** denotes observed log streamflow, **z** denotes observed soil moisture content, t denotes time. B is the mean of the priors of $(k_1,k_2,k_3,k_4) = (350\,\text{mm}, 0.0001, 90\,\text{mm}, 1.7\,\text{days})$, with prior covariance matrix $V_B = \text{diag}(0.4, 2.0, 0.1, 0.2)$. α and β with subscripts are the parameters for the inverse gamma distributions, the priors for the observation and process variances.

We implemented MCMC in R (R Development Core Team, 2008) to simulate the joint posterior. The initial values for the water levels of the two storage components (soil moisture storage and routing storage) were estimated based on Edijatno *et al*. (1999). The MCMC algorithms included Gibbs sampling (Gelfand *et al*., 1990) and adaptive Metropolis–Hastings steps (Haario *et al*., 2001; Marshall *et al*., 2004) to draw samples alternatively from the conditional posteriors for each of the unknowns, including the latent variables, parameters, and variances (Clark and Bjønstad, 2004). The adaptive algorithm is characterized by a proposal distribution based on the estimated posterior covariance matrix of the parameters, which is updated automatically. The posterior covariance matrix is calculated based on past iterations.

Predictive distributions of soil moisture and stream flow were constructed based on the climate scenarios, by marginalizing over the posterior distribution. We randomly selected 3000 sets from MCMC chains and evaluated both variables, including variances. The changes in temperature and precipitation were randomly sampled from the fitted density distributions based on the ensemble quantiles of the CMIP3 dataset. This approach integrates over uncertainties in parameters, model, and data.

The more detailed description of the process and hierarchical model above, and how the joint posterior was derived can also be found in Wu *et al*. (2010).

RESULTS AND DISCUSSION

Predictions of streamflow under the baseline climate scenario

The model predicts streamflow between 1985 and 2004 at low elevations and between 1993 and 2004 at high elevations well (Figure 1). The Nash–Sutcliffe efficiency values (ranging from - ∞ to 1, the closer the efficiency to 1, the more accurate the model is) based on the daily medians of the predicted streamflow from the model and the observed daily streamflow is 0.70 for low elevations, and 0.82 for high elevations, showing that predicted medians are in good agreement with field measurements. Meanwhile the predicted posterior of streamflow captures the variability of measured streamflow well with the exception of extreme streamflow events (Figure 1 and Figure S3). Few Bayesian applications in hydrological models can simulate extreme flows well (Li *et al*., 2012). A Bayesian modularization method has been proposed to reduce the extreme flow's effect on the streamflow uncertainty assessment of hydrological models (Li *et al*., 2012), but we did not employ this method in the current study.

Predictions under the three climate change scenarios

From predictive distributions of daily soil moisture and streamflow, we calculated the percent difference between the three climate change scenarios and the baseline climate scenario for each season (i.e. spring, summer, fall, winter) at both low and high elevations. Then, we summarized the quantiles and mean of the daily difference.

Soil moisture. Based on the mean of daily change, soil moisture tends to decline in summer, fall, and spring under the three climate scenarios at both low and high elevations

DOI: 10.1002/hyp

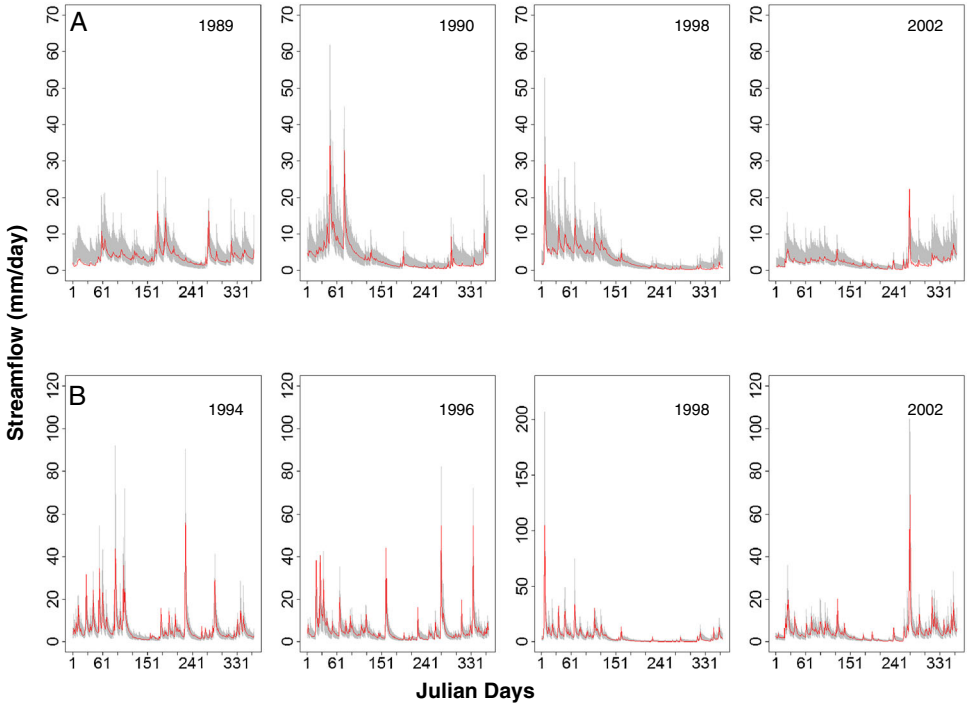

Figure 1. Observed daily streamflow (red lines) and 95% predictive intervals (grey area) from the hiearchical Bayesian models for selected years at low elevations (A) and high elevations (B). An extended comparison between observations and predictions for each year is shown in Figure S3

Table II. Quantiles and mean of percent change of soil moisture under the three climate scenarios compared to the baseline climate scenario at low and high elevations

Climate change scenarios	Seasons	Change of soil moisture (%)					
		Low elevations			High elevations		
		2.5% quantile	mean	97.5% quantile	2.5% quantile	mean	97.5% quantile
A2	Spring	−15.8	−5.53	0.803	−8.57	−2.33	1.42
	Summer	−23.6	−12.8	−1.19	−10.6	−3.23	0.199
	Fall	−23.4	−7.83	1.01	−7.26	−1.50	0.982
	Winter	−8.18	−1.96	1.73	−0.87	0.659	2.95
A1B	Spring	−15.1	−4.69	1.13	−6.08	−1.22	1.64
	Summer	−23.7	−12.1	−0.512	−8.41	−2.45	0.284
	Fall	−20.1	−7.74	0.93	−6.55	−1.46	0.715
	Winter	−8.40	−2.12	1.60	−0.944	0.564	2.61
B1	Spring	−1.10	−0.0929	0.710	−4.85	−0.822	1.34
	Summer	−1.65	−0.791	0.0675	−5.59	−1.21	0.673
	Fall	−1.14	−0.356	0.129	−4.60	−0.969	0.538
	Winter	−0.0807	0.234	1.72	−0.699	0.498	1.91

(Table II). The most pronounced decline occurs in summer followed by fall. Declines are greatest under the A2 scenario followed by the A1B scenario. Average declines are generally less than 10% except in summer under the A2 and A1B scenarios at low elevations. With uncertainties taken into consideration, soil moisture tends to decline in summer and fall under the three climate change scenarios at both low and high elevations. Under the B1 scenario, the 95% predictive intervals of the change for all the seasons are smaller and closer to 0 compared to the other two climate change scenarios, indicating the change of soil moisture and its variability is smaller. Under the A1 and A1B scenarios, the absolute mean change and the uncertainty are larger at low elevations than at high elevations.

Based on the medians of daily change, soil moisture in summer and fall is lower than baseline on more than 75% of all days at both low and high elevations (Figure 2). In winter, it tends to increase, especially at high elevations and under the B1 scenario. Overall, the most severe drying trend occurs in summer under the A2 scenario. High evapotranspiration, especially during the growing season, due to increased temperature, reduces soil moisture. Predicted increased precipitation contributes to increased soil moisture in winter under the B1 scenario. The changes of soil moisture are more refined under the B1 scenario compared to the A2 and A1B scenarios, largely due to the less variability in predictions of temperature and precipitation under the B1 scenario.

DOI: 10.1002/hyp

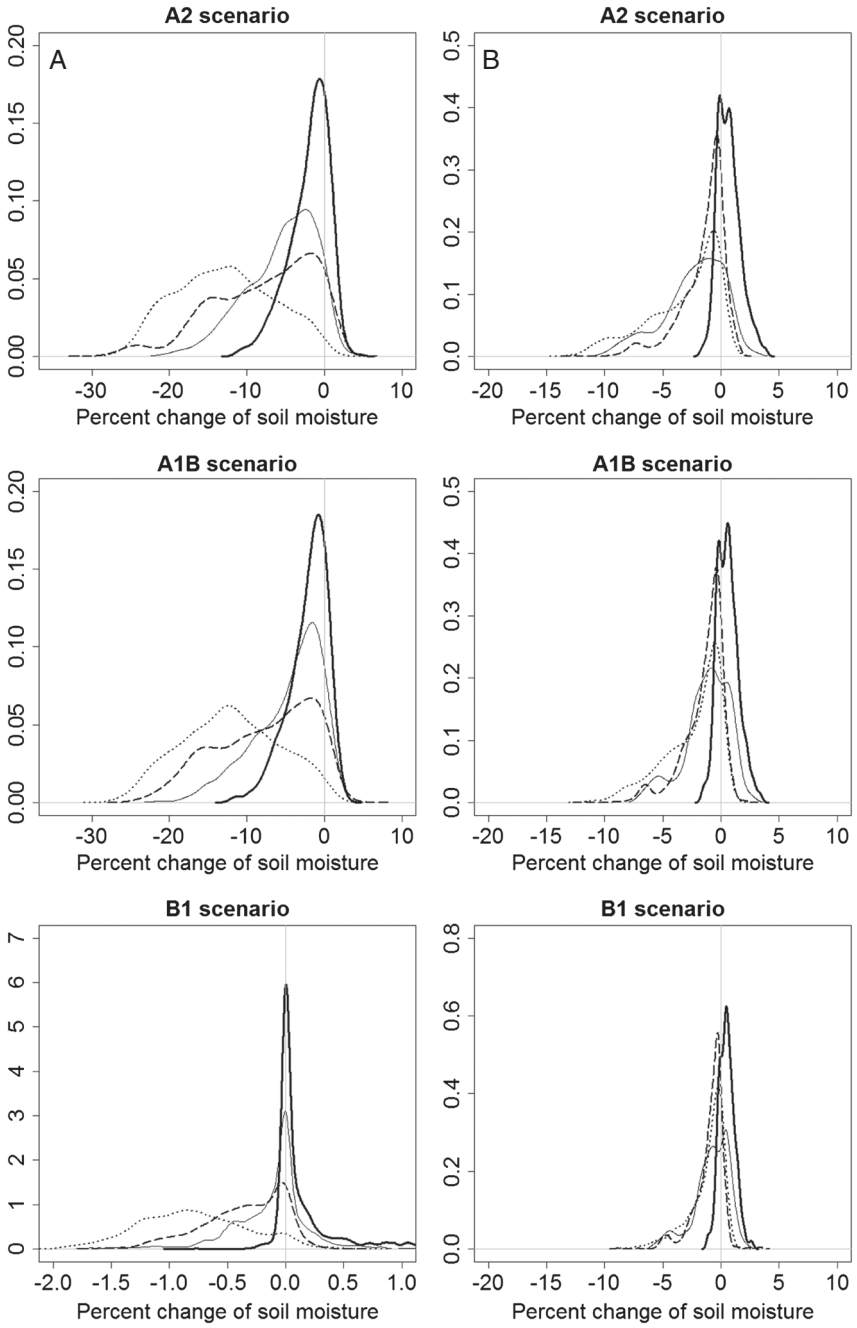

Figure 2. The probability distributions of median percent change of soil moisture between the three greenhouse gas emission scenarios and the baseline climate scenario for spring (black line), summer (dotted line), fall (dashed line), and winter (thick black line) at low (A) and high (B) elevations

Soil moisture provides a connection between physical processes at the catchment scale and biological processes at finer scales (Wu *et al*., 2010). It will not only affect subsurface streamflow (Kienzler and Naef, 2007) and saturation excess overland flow (van Meerveld and McDonnell, 2005), but also primary productivity, soil biogeochemical processes, and energy exchange between land and atmosphere (Hanson and Weltzin, 2000). Table III and Figure 3 show the 95% predictive intervals and probability distributions of days soil moisture levels are near the wilting point at both low (11% of volume, from soil survey geographic database SSURGO of Natural Resources Conservation Service, available at http://soils.usda.gov/survey/geography/ssurgo/, last accessed on April 6, 2012) and high elevations (9% of volume, from SSURGO). Days near the wilting point increase at both low and high elevations under changing climate. The drying trend is most pronounced under the A2 scenario.

Streamflow. Based on the means of daily change, streamflow at low elevations tends to decline in summer and fall under the A2 and A1B scenarios, with largest declines in summer under the A2 scenario (Table IV). At high elevations, streamflow tends to decline in summer under the A2 and A1B scenarios with the larger decline under the A2 scenario. The increase trend can be found in winter under all the climate change scenarios. Except for winter under the A2 and A1B scenarios at high elevations, the mean changes are

DOI: 10.1002/hyp

Table III. Quantiles of percent days soil moisture levels are near wilting point under different climate change scenarios at both low and high elevations

	Low elevations (% of days)			High elevations (% of days)		
Climate change scenarios	2.5% quantile	Median	97.5% quantile	2.5% quantile	Median	97.5% quantile
Baseline climate scenario	24.5	25.9	27.5	8.97	0.183	10.1
A2 emission scenario	28.0	29.5	30.9	12.1	0.593	13.1
A1B emission scenario	27.2	28.3	30.0	11.2	0.499	12.3
B1 emission scenario	25.6	27.0	28.6	10.3	0.267	11.3

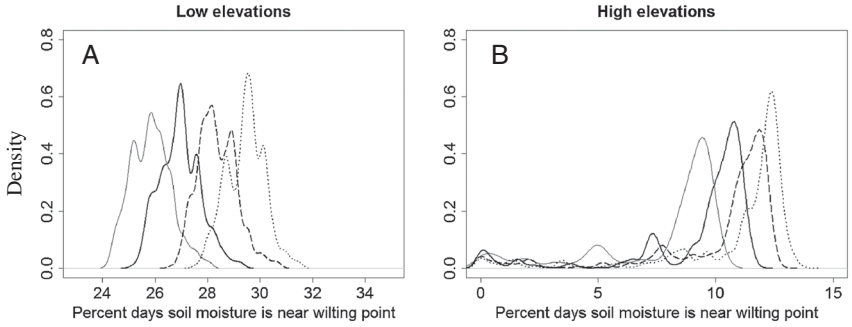

Figure 3. The probability distributions of percent days soil moisture is near wilting point under the baseline climate scenario (light black) and the three emission scenarios (dotted: A2; dashed: A1B; dark black: B1) at low (A) and high (B) elevations

Table IV. Quantiles and mean of percent change of streamflow under the three climate scenarios compared to the baseline climate scenario at low and high elevations

		Change of streamflow (%)					
		Low elevations			High elevations		
Climate change scenarios	Seasons	2.5% quantile	mean	97.5% quantile	2.5% quantile	mean	97.5% quantile
A2	Spring	−6.08	2.06	13.5	−14.3	−1.58	26.1
	Summer	−23.0	−7.49	1.78	−20.4	−6.99	0.115
	Fall	−24.2	−4.18	9.30	−12.5	1.16	12.5
	Winter	−2.46	8.07	22.45	−1.17	12.8	52.6
A1B	Spring	−1.56	5.73	15.7	−8.15	3.05	28.2
	Summer	−13.8	−1.62	7.36	−15.8	−3.55	3.89
	Fall	−17.46	−2.41	8.18	−11.5	0.296	9.47
	Winter	−1.60	6.85	21.46	−1.44	11.4	46.0
B1	Spring	0.419	4.04	10.6	−7.47	2.13	20.7
	Summer	−3.25	1.17	5.99	−9.41	0.112	6.47
	Fall	−4.48	0.738	4.94	−7.28	0.908	7.63
	Winter	1.69	5.17	14.4	−0.283	9.20	34.0

less than 10%. With uncertainties accounted for, streamflow in spring at low elevations and winter at both elevations shows significant increase under the B1 scenario, as its predictive intervals of the change are or very close to positive. Streamflow in summer, however, shows significant decrease under the A2 scenario at both low and high elevations, as its predictive intervals of the change are close to negative. Uncertainty of the percent change of streamflow (95% credible interval) is more than that of soil moisture for each season, especially at high elevations.

From the analysis on the medians of daily change, streamflow declines under the A2 and A1B scenarios on more than 60% of days in summer (Figure 4). Streamflow tends to increase under the B1 scenario with the largest increase being in winter and spring. The most severe drought trend would occur in summer under the A2 scenario at both low and high elevations. Streamflow increases on more than 90% of days across the three climate change scenarios in winter at both low and high elevations. More days show increases in streamflow in winter under the B1 emission scenario than under the other two climate change scenarios.

In summary, A2 emission scenario and A1B emission scenario show drier summers with less streamflow at both

DOI: 10.1002/hyp

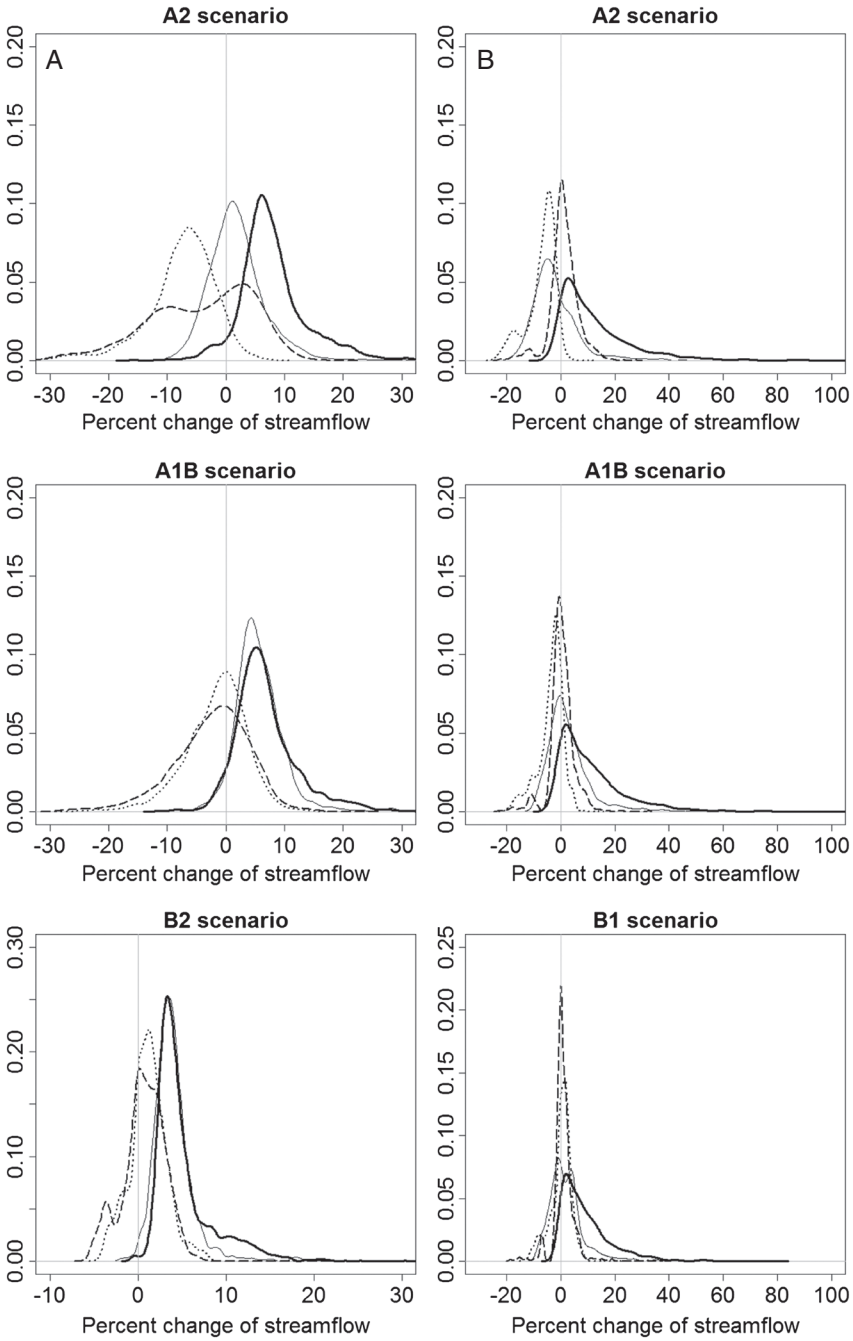

Figure 4. The probability distributions of median percent change of streamflow between the three greenhouse gas emission scenarios and the baseline climate scenario for spring (black line), summer (dotted line), fall (dashed line), and winter (thick black line) at low (A) and high (B) elevations

low and high elevations. Under those two emission scenarios, dying soils in spring are followed by even drier soil moisture and reduced streamflow in summer. Under the B1 scenario, streamflow in summer shows slightly increase. Streamflow tends to increase in winter across all the climate changes scenarios at both low and high elevations.

The effect of temperature versus precipitation on streamflow. To understand the relative contributions of changes in precipitation *versus* temperature on streamflow, we compared streamflow for scenarios with changes in temperature or precipitation alone to the baseline climate scenario. Precipitation and temperature changes were found to have similar impact on median changes of streamflow (Table V), with a slightly larger impact from precipitation at low elevations and a slightly larger impact from temperature at high elevations in general. With precipitation change alone, streamflow shows an overall increase, and it contributes to high extremes in streamflow. With temperature change alone, streamflow shows an overall decrease, and it contributes to low extremes in streamflow.

Whether streamflow is more sensitive to precipitation or to temperature depends on soils, vegetation, and most importantly, the climatic regime of the region. In cool regions, increased temperature may have a large impact. For example, streamflow could be substantially more sensitive to temperature than to precipitation in Hudson Bay in Canada (Waggoner, 1991). However streamflow is expected

DOI: 10.1002/hyp

Table V. Quantiles of percent change of streamflow with temperature change only or precipitation change only under the three climate change scenarios compared to the baseline climate scenario

Climate change Scenarios	Quantiles	Low elevations (%)		High elevations (%)	
		Precipitation change only	Temperature change only	Precipitation change only	Temperature change only
A2 scenario	2.5% quantile	0.625	−29.8	0.623	−22.8
	Median	8.65	−8.45	4.45	−5.93
	97.5% quantile	24.35	6.68	15.18	5.42
A1B scenario	2.5% quantile	3.14	−24.1	1.04	−19.9
	Median	9.98	−6.69	5.53	−4.97
	97.5% quantile	21.9	6.52	14.0	6.68
B1 scenario	2.5% quantile	3.31	−13.4	−0.201	−6.54
	Median	6.95	−4.08	0.460	−0.88
	97.5% quantile	13.0	4.60	2.82	1.23

to be more sensitive to precipitation than temperature in some dry areas in Australia, China, and Japan (Chiew *et al*., 1995; Guo *et al*., 2002; Tanakamaru and Kadoya, 1993). In a temperate humid climate like Coweeta basin where neither temperature nor precipitation is low, streamflow is likely to respond to changes in precipitation and temperature at a similar magnitude.

Implications for management and additional uncertainty. The Little Tennessee Basin (1797 mi2), into which our study areas drain, has experienced significant population growth and increased demand of freshwater resources for municipal – industrial – recreational – agricultural uses. Changes in streamflow generation in headwater catchments could have important implications downstream. The prediction of dry soils and reduced summer streamflow suggests that water resource managers will be challenged to meet the demands of a rapidly growing population for drinking water when water resources are needed the most. The potential for wetter winters may also challenge management for flood protection.

Additional uncertainty could be introduced when we applied the calibrated models based on the data from the baseline scenarios to the future scenarios of climate change, since the parameters may shift when conditions change (Merz *et al*., 2011). At Coweeta Basin, dry summers and wet autumns have become more frequent since the 1980s, consistent with the trend across the southeast US [Laseter *et al*., 2012; Angert *et al*., 2005; Groisman *et al*., 2004). Our HB model predicted reduced summertime soil moisture and streamflow by the end of the century, consistent with the observed trend. In addition, our model simulated streamflow well from 1940s to 2000s during which time some of the recent extreme climatic conditions have been observed. The Nash–Sutcliffe efficiency values based on the daily medians of the predicted streamflow from the model, and the observed daily streamflow is 0.73 for low elevation (1945–2004), and 0.80 for high elevation (1960–2004), showing that predicted medians are in good agreement with field measurements (Figure 5). 95% of predictive intervals from the model simulations generally intercepted the 1:1 line in the figure of model simulations *versus* observations (predictive intervals not shown here for clarity of the figure), indicating that the simulated streamflow captured the variability of observed streamflow at a daily base. These indicate that our model may be robust to the shift of climate and applicable to future climate scenarios. However, addressing the parameter shift under changing climate and hydrological regimes would potentially improve the model.

CONCLUSION

We have applied a parsimonious hydrological model in the HB framework to evaluate the potential impact of changing climate on soil moisture and streamflow at headwaters in the southern Appalachian Mountains. Although the model is

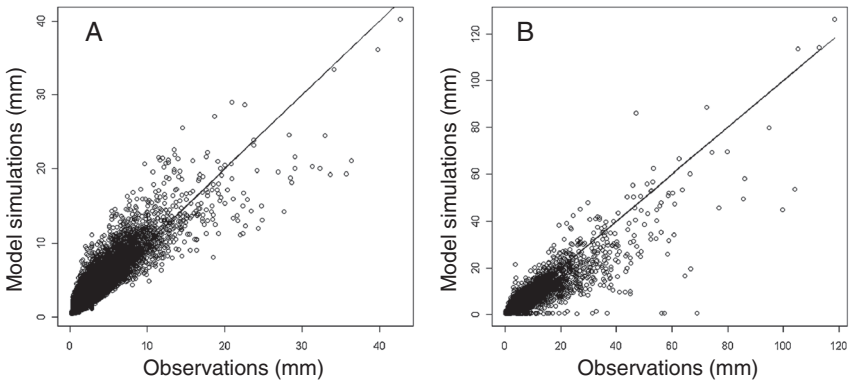

Figure 5. Medians of simulated daily streamflow vs. daily observations at low (A) and high elevations (B) (The blackline is 1:1 line. The closer the points to the line, the closer the similated medians to the observations, the better the model predictions)

DOI: 10.1002/hyp

coarsely parameterized, we are able to account for the major uncertainties from different sources. The most pronounced change in soil moisture and streamflow would occur under the A2 scenario at both low and high elevations, followed by the A1B scenario and then by the B1 scenario. Uncertainty of the change of soil moisture is less than that of streamflow for each season, especially at high elevations. A reduction of soil moisture in summer and fall, a reduction or a marginal increase of streamflow in summer, and an increase of streamflow in winter have been generally derived across the three climate change scenarios compared to the baseline climate scenario at both low and high elevations.

Informed decisions about managing water resources will require accurate and reliable predictions of future conditions. HB models integrating multiple long-term data sets with scenarios of future change provide full predictive distributions with the major uncertainties from different sources accounted for. Compared to deterministic point estimates, the richer information from full distributions in addition to mean and median estimates, can be reliable basis for a more informed sustainable water resource management, helping resource managers anticipate hydrological change under climate change and adapt more effectively to climate change to ensure water security.

ACKNOWLEDGEMENTS

This research was made possible by grants from the National Science Foundation through Coweeta Long Term Ecological Research (LTER). We thank USDA-Forest Service Coweeta Hydrologic Laboratory for the support of the data. We especially thank Drs. Chelcy Ford and Katherine Elliott at Coweeta Hydrological Laboratory for the insightful discussion on hydrological cycles at Coweeta basin. We also want to thank the editor and two anonymous reviewers for their helpful comments.

We acknowledge the modeling groups, the Program for Climate Model Diagnosis and Intercomparison and the World Climate Research Programme's (WCRP's) Working Group on Coupled Modelling for their roles in making available the WCRP CMIP3 multi-model dataset. Support of this dataset is provided by the Office of Science, U.S. Department of Energy. We especially want to thank Dr. Evan Girvetz at the Nature Conservancy for the valuable discussion on the climate change dataset.

REFERENCES

Ajami NK, Duan Q, Sorooshian S. 2007. An integrated hydrologic Bayesian multimodel combination framework: confronting input, parameter, and model structural uncertainty in hydrologic prediction. *Water Resources Research* **43**: W01403. DOI: 10.1029/2005WR004745.

Angert A, Biraud S, Bonfils C, Henning CC, Buermann W, Pinzon J, Tucker CJ, Fung I. 2005. Drier summers cancel out the CO_2 uptake enhancement induced by warmer springs. *Proceedings of the National Academy of Sciences* **102**: 10823–10827.

Barnett TP, Pierce DW, Hidalgo HG, Bonfils C, Santer BD, Das T, Bala G, Wood AW, Nozawa T, Mirin AA, Cayan DR, Dettinger MD. 2008. Human-induced changes in the hydrology of the western United States. *Science* **319**: 1080–1083.

Bates BC, Campbell EP. 2001. A Markov chain Monte Carlo scheme for parameter estimation and inference in conceptual rainfall-runoff modeling. *Water Resources Research* **37**(4): 937–947.

ter Braak CJF, Vrugt JA. 2008. Differential Evolution Markov Chain with snooker updater and fewer chains. *Statistics and Computing* **18**: 435–446.

Calder K, Lavine M, Mueller P, Clark JS. 2003. Incorporating multiple sources of stochasticity in population dynamic models. *Ecology* **84**: 1395–1402.

Campbell EP, Fox DR, Bates BC. 1999. A Bayesian approach to parameter estimation and pooling in nonlinear flood event models. *Water Resources Research* **35**(1): 211–220.

Chiew FHS, Whetton PH, McMahon TA, Pittock AB. 1995. Simulation of the impacts of climate change on runoff and soil moisture in Australian catchments. *Journal of Hydrology* **167**: 121–147.

Chiew FHS, Young WJ, Cai W, Teng J. 2011. Current drought and future hydroclimate projections in southeast Australia and implications for water resources management. *Stochastic Environmental Research and Risk Assessment* **25**, 601–612.

Clark JS. 2005. Why environmental scientists are becoming Bayesians. *Ecology Letters* **8**: 2–14. DOI: 10.1111/j.1461-0248.2004.00702.x.

Clark JS, Bjønstad ON. 2004. Population time series: process variability, observation errors, missing values, lags, and hidden states. *Ecology* **85**(11): 3140–3150.

Clark JS, Carpenter SR, Barbar M, Collins S, Dobson A, Foley JA, Lodge DM, Pascual M, Pielke Jr. R, Pizer W, Pringle C, Reid WV, Rose KA, Sala O, Schlesinger WH, Wall DH, Wear D. 2001. Ecological forecasts: an emerging imperative. *Science* **293**: 657–660.

Clark JS, Agarwal P, Bell DM , Flikkema P, Gelfand A, Nguyen X, Ward E, Yang J. 2011. Inferential ecosystem models, from network data to prediction. *Ecological Applications* **21**: 1523–1536.

Edijatno, Nascimento NO, Yang X, Makhlouf Z, Michel C. 1999. GR3J: a daily watershed model with three free parameters. *Hydrological Sciences Journal* **44**(2): 263–277.

Gedney N, Cox PM, Betts RA, Boucher O, Huntingford C, Stott PA. 2006. Detection of a direct carbon dioxide effect in continental river runoff records. *Nature* **439**: 835–838.

Gelfand AE, Hills SE, Racine-Poon A, Smith AFM. 1990. Illustration of Bayesian inference in normal data models using Gibbs sampling. *JASA* **85**: 972–985.

Girvetz EH, Zganjar C, Raber GT, Maurer EP, Kareiva P, Lawler JJ. 2009. Applied climate-change analysis: the climate wizard tool. *PLoS One* **4** (12): e8320. DOI: 10.1371/journal.pone.0008320

Gleick PH. 1987. Regional hydrologic consequences of increases in atmospheric CO_2 and other trace gases. *Climatic Change* **10**: 137–160.

Gosling SN, Warren R, Arnell NW, Good P, Caesar J, Bernie D, Lowe JA, van der Linden P, O'Hanley JR, Smith SM. 2011. A review of recent developments in climate change science. Part II: The global-scale impacts of climate change. *Progress in Physical Geography* **35**(4): 443–464.

Groisman PY, Knight RW. 2008. Prolonged dry episodes over the conterminous United States: new tendencies emerging during the last 40 years. *Journal of Climate* **21**: 1850–1862.

Groisman PY, Knight RW, Karl TR, Easterling DR, Sun B, Lawrimore JH. 2004. Contemporary changes of the hydrological cycle over the contiguous United States: trends derived from in situ observations. *Journal of Hydrometeorology* **5**: 64–85.

Guo S, Wang J, Xiong L, Ying A, Li D. 2002. A macro-scale and semi-distributed monthly water balance model to predict climate change impacts in China. *Journal of Hydrology* **268**: 1–15.

Haario H, Saksman E, Tamminem J. 2001. An adaptive metropolis algorithm. *Bernoulli* **7**(2): 223–242.

Hanson P, Weltzin JF. 2000. Drought disturbance from climate change: response of United States forests. *The Science of the Total Environment* **262**: 205–220.

Hatcher Jr. RD. 1979. The Coweeta Group and Coweeta syncline: major features of the North Carolina - Georgia Blue Ridge. *Southeastern Geology* **21**(1): 17–29.

Hatcher Jr. RD. 1988. Bedrock geology and regional geologic setting of Coweeta Hydrologic Laboratory in the eastern Blue Ridge. In *Forest Hydrology and Ecology at Coweeta, Ecological Studies*, vol. **66**, Swank, WT, Crossley Jr. DA (eds). Springer-Verlag: New York; 81–92.

IPCC (Intergovernmental Panel on Climate Change). 1996. *Climate change 1995: The science of climate change*. Cambridge University Press: Cambridge, UK; 529.

Jackson CH. 2011. Multi-State Models for Panel Data: The msm Package for R. *Journal of Statistical Software* **38**(8): 1–29. URL http://www.jstatsoft.org/v38/i08/.

Jackson RB, Carpenter SR, Dahm CN, McKnight DM, Naiman RJ, Postel SL, Running SW. 2001. Water in a changing world. *Ecological Applications* **11** (4): 1027–1045.

Jakeman AJ, Hornberger GM. 1993. How much complexity is warranted in a rainfall-runoff model? *Water Resources Research* **29**: 2637–2649.

Kienzler PM, Naef F. 2007. Temporal variability of subsurface stormflow formation. *Hydrology and Earth System Sciences and Discussions* **4**: 2143–2167.

Kilsby CG, Tellier SS, Fowler HJ, Howels TR. 2007. Hydrological impacts of climate change on the Tejo and Guadiana Rivers. *Hydrology and Earth System Sciences* **11**(3): 1175–1189.

Kleinen T, Petschel-Held G. 2007. Integrated assessment of changes in flooding probabilities due to climate change. *Climatic Change* **81**: 283–312.

Krzysztofowicz R. 1999. Bayesian theory of probabilistic forecasting via deterministic hydrological model. *Water Resources Research* **35**(9): 2739–2750.

Kuczera G, Mroczkowski M. 1998. Assessment of hydrologic parameter uncertainty and the worth of multiresponse data. *Water Resources Research* **34**: 1481–1489.

Kuczera G, Parent E. 1998. Monte Carlo assessment of parameter uncertainty in conceptual catchment models: the metropolis algorithm. *Journal of Hydrology* **211**: 69–85.

Kundzewicz ZW, Mata LJ, Arnell NW, Döll P, Kabat P, Jiménez B, Miller KA, Oki T, Sen Z, Shiklomanov IA. 2007. Freshwater resources and their management. In *Climate Change 2007: Impacts, Adaptation and Vulnerability. Contribution of Working Group II to the Fourth Assessment Report of the Intergovernmental Panel on Climate Change*, Parry ML, Canziani OF, Palutikof JP, van der Linden PJ, Hanson CE (eds). Cambridge University Press: Cambridge, UK; 173–210.

Laseter SH, Ford CR, Vose JM, Swift Jr. LW. 2012. Long-term temperature and precipitation trends at the Coweeta Hydrologic Laboratory, Otto, North Carolina, USA. *Hydrology Research* **43**(6): 890–901.

Li L, Xu C-Y, Engeland K. 2012. Development and comparison of Bayesian modularization method in uncertainty assessment of hydrological models. *Geophysical Research Abstracts* **14**: EGU2012-1897.

Loukas A, Vasiliades L, Dalezios NR. 2002. Climatic impacts on the runoff generation processes in British Columbia, Canada. *Hydrology and Earth System Sciences* **6**(2): 211–228.

Marshall L, Nott D, Sharma A. 2004. A comparative study of Markov chain Monte Carlo methods for conceptual rainfall-runoff modeling. *Water Resources Research* **40**. DOI: 10.1029/2003WR002378.

van Meerveld IT, McDonnell JJ. 2005. Comment to "Spatial correlation of soil moisture in small catchments and its relationship to dominant spatial hydrological processes, Journal of Hydrology 286, 113–134". *Journal of Hydrology* **303**: 307–312.

Merz R, Parajka J, Blöschl G. 2011. Time stability of catchment model parameters: implications for climate impact analyses. *Water Resources Research* **47**: W02531. DOI: 10.1029/2010WR009505, 2011.

Meybeck M, Vörösmarty CJ. 2004. Part D. IGBP Global Change Series. In *Vegetation, Water, Humans and the Climate: A New Perspective on an Interactive System*, Kabat P, Claussen M, Dirmeyer PA, Gash JHC, de Guenni LB, Meybeck M, Pielke R, Vörösmarty CJ, Hutjes RWA, Lütkemeier S (eds). Spring-Verlag: Berlin; 294–480.

Nakiénovic N, Alcamo J, Davis G, de Vries D, Fenhann J *et al*. 2000. Special Report on Emissions Scenarios. A Special Report of Working Group III of the Intergovernmental Panel on Climate Change. Intergovernmental Panel on Climate Change (Eds). Cambridge, UK, Cambridge University Press.

Neilson RP, Marks D. 1994. A global perspective of regional vegetation and hydrologic sensitivities from climatic change. *Journal of Vegetation Science* **5**: 715–730.

Ohmura A, Wild M. 2002. Is the hydrological cycle accelerating? *Science* **298**: 1345–1346.

Oki T, Kanae S. 2006. Global hydrological cycles and world water resources. *Science* **313**: 1068–1072.

Palmer MA, Liermann CAR, Nilsson C, Flörke M, Alcamo J, Lake PS, Bond N. 2008. Climate change and the world's river basins: anticipating management options. *Frontiers in Ecology and the Environment* **6**(2): 81–89. DOI: 10.1890/060148.

Penninckx V, Meerts P, Herbauts J, Gruber W. 1999. Ring width and element concentrations in beech (*Fagus sylvatica* L.) from a periurban forest in central Belgium. *Forest Ecology and Management* **113**: 23–33.

Perrin C, Michel C, Andréassian V. 2003. Improvement of a parsimonious model for streamflow simulation. *Journal of Hydrology* **279**: 275–289.

R Development Core Team. 2008. *R: A language and environment for statistical computing*, R Foundation for Statistical Computing: Vienna, Austria. ISBN 3-900051-07-0, URL http://www.R-project.org.

Schneider SH. 2001. What is "dangerous" climate change? *Nature* **411**: 17–19.

Sivakumar B. 2011. Global climate change and its impacts on water resources planning and management: assessment and challenges. *Stochastic Environmental Research and Risk Assessment* **25**: 583–600.

Swank WT, Crossley Jr. DA. 1988. Forest hydrology and ecology at Coweeta. In *Ecological Studies*, Vol. **66**, Swank WT, Crossley Jr. DA (eds). Springer-Verlag: New York; 3–16.

Swift Jr. LW, Cunningham GB, Douglass LE. 1988. Climatology and hydrology. In *Forest Hydrology and Ecology at Coweeta*, Ecological Studies, vol. **66**, Swank, WT, Crossley Jr. DA (eds). Springer-Verlag: New York; 35–55.

Tanakamaru H, Kadoya M. 1993. Effects of climate change on the regional hydrological cycle in Japan. In *Exchange processes at land surface for a range of space and time scales: proceedings of an international symposium held at Yokohama*, **55**, Bolle HJ, Feddes RA, Kalma JD (eds). Japan, 13-16 July, IAHS: Wallingford, UK; 535–542.

Vörösmarty CJ, Green P, Salisbury J, Lammers RB. 2000. Global water resources: vulnerability from climate change and population growth. *Science* **289**: 284–288.

Vrugt JA, Robinson A. 2007. Treatment of uncertainty using ensemble methods: comparison of sequential data assimilation and Bayesian model averaging. *Water Resources Research* **43**: W01411. DOI: 10.1029/2005WR004838.

Vrugt JA, Diks CG, Gupta HV, Bouten W, Verstraten JM. 2005. Improved treatment of uncertainty in hydrological modeling: combing the strengths of global optimization and data assimilation. *Water Resources Research* **41**: W01017. DOI: 10.1029/2004WR003059.

Vrugt JA, ter Braak CJF, Diks CGH, Schoups G. 2012 (in press). Hydrologic data assimilation and using particle Markov chain Monte Carlo simulation: theory, concepts and applications. *Advances in Water Resources*.

Waggoner PE. 1991. U.S. water resources versus an announced but uncertain climate change. *Science* **251**: 1002.

Wikle C. 2003. Hierarchical Bayesian models for predicting the spread of ecological processes. *Ecology* **84**(6): 1382–1394.

Wu W, Clark JS, Vose JM. 2010. Assimilating multi-source uncertainties of a parsimonious conceptual hydrological model using hierarchical Bayesian modeling. *Journal of Hydrology* **394**: 436–446.